Heterogeneous catalysis via light-heat dual activation: A path to the breakthrough in C1 chemistry

Bingqiao Xie, Di Hu, Priyank Kumar, Vitaly Ordomsky, Andrei Khodakov, Rose Amal

Heterogeneous Catalysis via Light-Heat Dual-Activation: A Path to the Breakthrough in C_1 Chemistry

Bingqiao Xie[1,3]*, Di Hu[2,4] Priyank Kumar[1], Vitaly V. Ordomsky[2], Andrei Y. Khodakov[2]*, Rose Amal[1]*

[1]School of Chemical Engineering, The University of New South Wales, Sydney, NSW 2052, Australia
[2]UCCS−Unité de Catalyse et Chimie du Solide, Université de Lille, CNRS, Centrale Lille, Université d'Artois, UMR 8181, F-59000Lille, France
[3]Group of Catalysis for Biofuels, École Polytechnique Fédérale de Lausanne, Lausanne, Switzerland
[4]Hubei Key Laboratory of Pollutant Analysis and Reuse Technology, College of Chemistry and Chemical Engineering, Hubei Normal University, Huangshi, Hubei 435002, China
*bingqiao.xie@epfl.ch/andrei.khodakov@univ-lille.fr/r.amal@unsw.edu.au

Context & scale

The alarming rise in global temperatures, attributed to excessive CO_2 emissions, has highlighted the imperative of developing innovative strategies and sustainable technologies for chemical production using renewable energy sources. One promising approach involves the utilization of light-heat dual-activation, wherein both photochemical and thermal catalytic pathways synergistically drive chemical reactions with exceptional performance, while minimizing the need for intensive heating.

This groundbreaking perspective introduces, for the very first time, a classification system aimed at systematically studying photothermal catalysis. Within each category, we conduct a thorough evaluation of their essential traits and the latest advancements at the forefront of the field. This evaluation aims to provide a better understanding of light-heat coupled catalytic systems and highlighting its strength in amplifying the efficiency of chemical synthesis, mainly in the scope of C1 chemistry. Furthermore, we identify and address the multifaceted challenges that arise in the pursuit of novel photothermal systems. These challenges encompass pioneering catalyst development, delving into mechanistic intricacies, and strategically designing advanced photoreactors. It becomes evident that the inherent advantage of the light-heat dual-activation system, as opposed to individual approaches, positions it as a pragmatic pathway towards realizing a more energy-efficient and sustainable production of future energy carriers and sought-after building-block chemicals.

Summary

A hybrid photothermal catalytic system, which combines both the photochemical (light) and thermal (heat) activation pathways over a bifunctional catalyst, has demonstrated remarkable levels of reaction activity and selectivity when compared to individual photo- and thermo- catalysis. However, the complex nature of the hybrid system, coupled with the synergy between photocatalysis and thermocatalysis, has made it challenging to understand (and thus manipulate) the role of individual stimuli (light/heat) and catalyst surface processes. In this perspective, systematic classification for different (complicated) photothermal catalysis reaction systems are provided. We evaluate the singular catalytic characteristics of each category, together with the competence of light-heat dual-activation in overcoming the well-defined limitations in photocatalysis and thermocatalysis, mainly in the scope of C1 chemistry. Notably, the interplay and cooperation among heat and/or light-induced effects can be engineered to greatly extend the capability of chemical transformation (i.e., product selectivity, reactivity) via well-established photo-thermo cascade reaction. Finally, we provide critical insights into the catalyst development and reactor design for high-performance light-heat coupled catalytic systems.

Graphical abstract

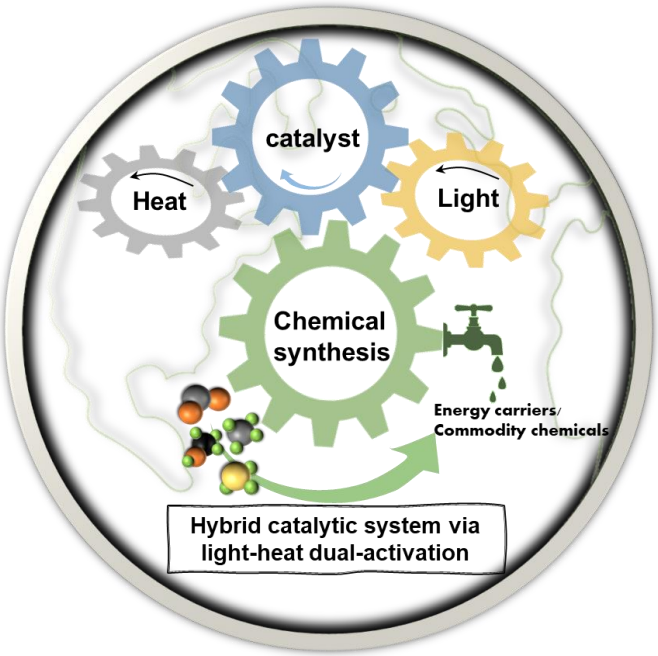

Keywords: photothermal catalysis, C1 chemistry, photocatalysis, solar fuels

1. Introduction

1.1. Background

Modern society is built upon a "carbon economy" where a significant number of goods are constructed using carbon-based materials. Inevitably, the sustainable utilization of alternative carbon feedstocks, including captured CO_2[1-2], alternative methane (derived from biogas or abundant and less carbon-intensive natural gas)[3-4] and biomass[5-6], in an efficient and greener approach will become more and more important for the supply of C-embedded fuels and chemicals in our daily life with the gradual phasing out of fossil fuels[7-8]. In addition, hydrogen, as an essential building block in the chemical industry, is taken as another important element in facilitating the transition from exhaustible fossil fuels to sustainable renewable sources. From a scientific research perspective, the exploration of more energy-efficient and sustainable chemical utilisation/transformation technologies (relevant to "Zero-Waste Economy", "Circular Carbon Economy" and "Hydrogen Economy") will play a key role in refining the structure of chemical industry for addressing the faced environmental issues and satisfying our ever-growing needs for energy and chemicals.

A large majority of chemical processes involves a catalyst. With different driving forces (e.g., light, heat, electricity, plasma), catalyst can be activated for the execution and acceleration of chemical transformation from abundant feedstocks to demanding chemicals/fuels to meet for our daily needs, if applicable, simultaneously storing the clean energy into stable chemical bonds (i.e., via endergonic reaction). Among different catalytic reaction systems, combination of heat and light has recently stand out as an alternative approach and technology to contribute to the circular carbon economy while unleash the potential of solar energy in chemical synthesis, especially in the scope of C1 chemistry where chemical utilisation of CO_2 is centred.

1.2. Thermocatalysis

Typically, to drive chemical reactions, thermal activation currently represents one of the most efficient and feasible strategies in industrial chemical synthesis. However, there are three common bottlenecks in this thermally driven catalytic process.

i) The energy efficiency of the process is limited by the fact that a significant amount of energy is expended in heating up surroundings and in driving undesired side reactions. If the process heating is provided by fossil energy feedstocks, thermocatalytic processes produce large amounts of CO_2, the main greenhouse gas.

ii) Second, the thermodynamics limits the reaction performance across the whole range of the operating conditions.

iii) Severe degradation in catalyst structure/active sites under harsh conditions requires a frequent catalyst replacement or regeneration which also account for high industrial operating cost.

It is worth emphasizing that operating at lower temperature provides several benefits, including (but not limited to) an increased catalyst lifetime, desirable thermodynamics, suppressed coking, restrained side-reactions and thus increased selectivity towards target products, etc. Taking methane conversion as an example, due to a strong C-H bond, high operation temperature is often required (>750 °C) which results in excessive energy consumption and serious coke formation/catalyst sintering[9]. In addition, direct selective activation and efficient conversion of methane via Methane Partial Oxidation (MPO) into other target compounds (i.e., methanol and higher hydrocarbons) are very challenging due to the high reactivity of these products compared to methane[10] and production of majors amounts of CO_2. To prevent the deep conversion/over-oxidation of the methane and isolate the targeted products, the reaction can be purposely conducted at the low-temperature region where the reactivity can be kinetically controlled. Therefore, to tackle these temperature-relevant limitations, the introduction of another driving force/activation pathway could be intently required to mitigate the dilemma encountered in thermally driven catalysis reactions.

1.3. Photocatalysis

Photocatalysis is a chemical process that uses abundant light energy to initiate and facilitate a chemical reaction mostly under room temperature. The absorbed light energy by a photocatalysts (normally a semiconductor) excites electrons (e^-) and holes (h^+), also called photogenerated charge carriers, that then migrate to the catalyst surface to interact with molecules and finally drive redox reactions. However, semiconductor-based photocatalysis encounters challenges:

i) lower reactivity/photonic efficiency. Factors such as limited light absorption, substantial surface/volume recombination of charge carriers, and reactant/product mass transport limitations contribute to low reactivity (often several orders of magnitude below thermal catalysis) and low photon-to-chemical efficiency in photocatalysis.

ii) lower selectivity. Photocatalytic transformations, like methane conversion, often follow radical mechanisms involving intricate reaction networks with multiple pathways. Consequently, semiconductor-involved reactions frequently exhibit inadequate selectivity toward the desired product.

iii) inefficient use of solar spectrum. Many conventional photocatalysts possess bandgap energies that restrict their absorption to a limited portion of the solar spectrum, primarily within the ultraviolet (UV) region. Consequently, a substantial portion of solar energy, especially within the visible and infrared regions, cannot be effectively harnessed to drive photocatalytic reactions.

1.4. Photothermal catalysis

A hybrid photothermal catalysis, which relies on the light-heat dual-activation, is nowadays estimated to be feasible in solving the challenges of conventional thermocatalysis and photocatalysis, and in extending the capability of chemical transformation (see Table S1 for more examples). The stimuli,

being heat or energetic charge carriers, is designated to drive the catalytic elementary steps in a synergetic and more efficient way. On the one hand, the coupled reactions take place at accelerated reaction rate or at an optimum temperature which is typically lower than in pure thermal conditions.[11-13]. On the other hand, although the performance delivered by state-of-art photocatalytic systems is far beyond being sufficient (i.e., restricted by the poor catalyst activity, selectivity, and/or low photonic efficiency), the temperature, which is often reckoned irrelevant or detrimental to photocatalysis due to the suppressed adsorption of reactant[14] or increased electron-holes recombination[15], has been found beneficial for a group of gaseous (plasmonic) photocatalysis[15-18]. Furthermore, the exploration of dedicated cooperation between photocatalysis and thermocatalysis has invoked a new catalytic system that can unlock unique reaction pathways, potentially, for the synthesis of more valued products.

This perspective focuses on the emerging field of hybrid catalytic systems where both heat and light act collaboratively to drive the chemical reactions. Significantly, we explore the potential/opportunities of light-heat dual-activation in further extending the capability (energy efficiency, productivity, selectivity, etc.) of important heterogeneous catalytic reactions. We hope that this perspective will inspire researchers on the design of innovative catalytic systems where synergism between heat- and light-induced chemistries can be maximized, ultimately translating into solutions for more energy-efficient and sustainable chemical production of future energy carriers and highly demanded building-block chemicals.

2. Heterogeneous catalysis under light-heat dual-activation

The hybrid catalytic systems driven by light-heat dual-activation exploit typically the synergy between thermal activation and light-induced effects. The presence of these synergistic effects has, however, made it challenging to study/understand, and thus manipulate, the role of individual stimuli (light/heat) and catalyst surface processes. In this section, a classification system for photothermal catalysis is proposed based on the relative contribution of thermal and nonthermal effects initiated by light illumination, as well as the dominant mechanism involved (photocatalysis or thermocatalysis).

2.1. Thermal and nonthermal effects followed by light-matter interaction

Followed by the optical excitation of a substrate/adsorbate system, both thermal and nonthermal effects can be induced along with the nonradiative energy dissipation pathway (Figure 1a). Thermal effects, or light-induced heating, refer to the heating of the substrate accompanied by the dissipation of adsorbed photonic energy into the lattice (via electron-phonon coupling). Nonthermal effects, which might be beneficial for chemical reactions, are normally associated with charge/energy exchange between the substrate and chemically attached entities or local electromagnetic field enhancement at the surfaces of plasmonic nanostructures.[19-21].

In a substrate/adsorbate system, the nonthermal chemical effects associated with the decay of optical excitation (e.g., SPR or band-gap excitation) can be broadly divided into a) the perturbation of the chemical state of substrate/adsorbate system (i.e., creating transient negative ions (TNIs)[22-23]) with the electron-mediated transient energy exchange, b) stimulating surface catalytic redox reactions with charge carriers being consumed, and c) regulating catalyst surface state. For case b, photogenerated charge carriers can provide dominant or even exclusive energy for surface chemical reactions (i.e., semiconductor and plasmonic photocatalysis). For case a, however, the photogenerated charge carriers are considered unapt of driving the complex multi-step catalytic reactions (for example, significant thermal activation/contribution is needed) but able to regulate/disturb the adsorbate (e.g., electronically or vibrationally excited). These charge-mediated disturbing effects would initiate for example polarisation and desorption of molecules, which could finally contribute to the successive process (chemical reactions or product desorption), if necessary, with the assistance of heat[24-28].

The measures to estimate the ratio of contributions for light-induced thermal and nonthermal effects can be classified into following three categories: i) direct measurement of detectable signals (e.g.,

advanced measurement techniques (IR camera[29] or ultrafast Raman thermometry[30] for the measurement of localised heating and spectroscopical characterisation of charge transfer process[31]); ii) design of comparative experiments[32] based on the different characters of two activation mechanisms (i.e., wavelength-dependency, light-intensity dependency, effective penetration depth[33]); iii) Mathematics calculation (e.g., the calculation of local temperature based on thermodynamic parameters and observed activity[34]). Applicable measures can be highly dependent on the nature of the studied catalytic system (i.e., reactor/catalyst geometry, reaction, temperature range). It is recommended that multiple strategies are employed to evaluate or quantify the relative contributions of thermal and nonthermal effects.

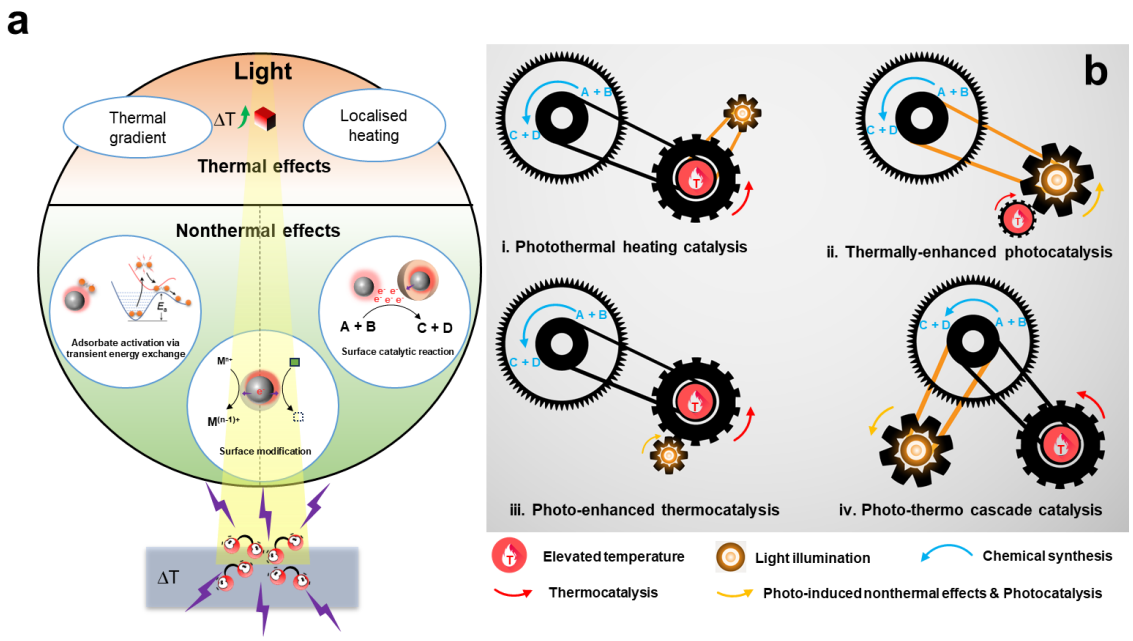

Figure 1. Driving forces and classification of photothermal catalysis (a)Thermal and nonthermal effects followed by the light-matter interaction. The unique light-induced thermal effects, including thermal gradient and localised heating, could trigger different catalytic behaviours compared to conventional electric heating. Photogenerated charge carriers are able to alter the character of adsorbed species and catalyst surface state (so called nonthermal effects) to further modify/improve catalytic performance (b) Schematic illustration of four discrete categories of photothermal catalysis, organized based on the prevailing influence and relative participation of thermal and nonthermal (photo-activation) effects. These effects constitute the primary driving forces for photothermal catalytic chemical conversions from initial reactants (A+B) to ultimate products (C+D).

2.2. Classifications of photothermal catalysis

Since photothermal catalysis represents a very broad definition of reactions where heat and light both participate, it is important to classify them before going into the discussion of any specific example. We found it practical to classify based on how the thermal activation and photo-activation cooperate with each other in the reaction. As shown in Table 1 and Figure 1b. photothermal catalysis can be divided into four categories.

(i) **Photothermal heating catalysis**. Photothermal heating catalysis, or light-driven thermocatalysis, is a class of reaction which is solely driven by the light-induced heating effect. Though these reactions behave similar to thermocatalysis in detailed activation mechanism and reaction pathway, different reaction behaviours (enabled by the atypical feature of light-induced heating) could be observed and will be discussed below.

(ii) **Thermally-enhanced photocatalysis.** represents another class of photothermal catalysis that rational heating is utilised to accelerate the photocatalytic reaction rate.

(iii) **Photo-enhanced thermocatalysis.** where photo-generated charge carriers play an assisting role in a thermocatalysis-dominated reaction pathway. In this case, photogenerated charge carriers from semiconductor/metal act to modify the surface catalyst surface states or accelerate the surface intermediary steps, leading to increased activity.

(iv) **Photo-thermo cascade catalysis.** Lastly, there is another type of photothermal reactions that emphasize the progressive cooperation between photocatalysis and thermocatalysis, and targeted reaction pathways and products can be achieved only when surface reactivity is simultaneously coupled with photocatalytic steps

Table 1. Classification of photothermal catalysis and corresponding characteristics/features.

Category	Subdivision/description	Reaction driving forces	Key aspects for mechanistic understanding	Performance vs. single activation approach	Examples
Photothermal heating catalysis	Light-driven thermocatalysis	Photo-induced heating	1. *Light-to-heat conversion;* 2. *Localised heating/thermal gradient;*	Same or better than thermocatalysis	● Ammonia synthesis over $TiO_{2-x}H_y/Fe$[35]
Thermally-enhanced photocatalysis	High-temperature plasmonic photocatalysis	Plasmonic excitation (main) Thermal activation (promotion)	1. *Activity dependency on temperature and light intensity;* 2. *Catalyst Debre temperature;* 3. *Electron-hole recombination at elevated temperature;*	Negligible activity under thermal-only condition **&** Improved Photocatalytic activity under moderate heating;	● AuPt bimetallic nanoparticles for CO_2 hydrogenation[36] ● Photocatalytic CO_2 reduction on plasmonic Bi_2O_{3-x}[37]
	High-temperature semiconductor photocatalysis	Bandgap excitation (main) Thermal activation (promotion)			● Black indium oxide for CO_2 reduction[38] ● Ag-ZnO/TiO_2 for Methane oxidative coupling[17]
Photo-enhanced thermocatalysis	Plasmon-enhanced thermocatalysis	Thermally-driven chemistry (main) Plasmon-induced activation (promotion)	1. *Activity dependency on temperature and light intensity;* 2. *Operando probing of catalyst surface chemistry/intermediates under light;* 3. *Kinetic analysis (apparent activation energy barrier);* 4. *Electron transfer pathways;*	Noticeable activity under thermal-only condition **&** Increased activity and/or selectivity upon illumination **&** Lowered apparent activation energy barrier **&** lowered onset reaction temperature	● Plasmonic CuZn alloy for methanol reforming[39] ● Rh/Al_2O_3 for CO_2 hydrogenation
	Bandgap excitation enhanced thermocatalysis	Thermally-driven chemistry (main) Bandgap excitation (promotion)			● MgO/Pt/Zn-CeO_2 for dry reforming of methane[40]
	Dual/Multiple-excitation enhanced thermocatalysis	Thermally-driven chemistry (main) Plasmonic and bandgap excitation (synergistic promotion)			● Cu/ZnO/Al_2O_3 for methanol synthesis from CO_2[41] ● Cu/Zn/Zr oxide nanocatalyst for methanol reforming[42]
Photo-thermo cascade catalysis	Coupling of photocatalysis with thermocatalysis	Photochemistry + thermochemistry	1. *Individual reaction mechanism/pathway in photocatalysis and thermocatalysis* 2. *Cooperation between photocatalysis and thermocatalysis;*	New product might be yielded with coupled mechanism/pathway	● CO_2 reduction with H_2O over Cu/ZnO&Pt-$K_2Ti_6O_{13}$[43] ● CO hydrogenation over Cu-Co/$SrTiO_3$[44]

2.3. Photothermal heating catalysis

On a strong light-absorbing nanostructure catalyst, significant light-induced heating (built up to several hundred Celsius degree under low-intensity illumination) can be directly harnessed to initiate important reactions like CO_2/CH_4 conversion[45-46], N_2 reduction[47], and methanol dehydrogenation[48]. To improve the energy efficiency of photothermal heating catalysis, the focus of this field lies on the one hand, on the effective light focusing/guiding technology and the materials engineering strategies which could effectively enhance heat generation and simultaneously reduce heat loss in a catalyst- reactor system[34, 49]. On the other hand, given the unique heat generation/dissipation process within materials under illumination, which could lead to localized heating or thermal gradient across the catalytic geometry, light-induced heating may act differently compared to electric heating when it is employed to drive catalytic reactions. The local temperature distribution at the micro-level can be studied with experimental approaches (i.e., multi-point temperature measurement[35], thermal imaging camera[50], temperature-sensitive spectroscopic probing[51-52]) and theoretical simulation/calculation method[52-53]. Intuitively, the thermal gradient can be designed to purposely catalyse relay catalysis, which involves at least two reactions. The first one favours high temperature and the second favours low temperature. Mao et al. reported a dual-temperature-zone catalysis (DTZC) enabled by light-induced local heating, where high-temperature N_2 activation and low-temperature NH_3 formation were spatially separated at "hot" Fe and "cool" $TiO_{2-x}H_y$, respectively[52]. In this way, the reaction is no longer limited by the traditional thermodynamic equilibrium. A high ammonia yield/catalytic efficiency were achieved. This strategy perfectly circumvents the dilemma between the kinetics and thermodynamics in conventional exothermic reactions. In addition, the direction of thermal gradient under either conventional heating or light illumination has been demonstrated by Li et al. to have a significant influence on the catalytic ammonia production over ruthenium catalysts[35]. Different to the reactions under isothermal conditions that are limited by the equilibrium constant curve ($Q_P \leqslant K_{iso}$), the non-isothermal conditions showed an unusual $Q_P > K_{iso}$ for a given $T_e > 450$ °C and the measured N_2 conversion is nearly 50% larger than the calculated equilibrium conversion at $T_e = 500$ °C (insert of Figure 5b). This has been correlated to the fact that molecules tend to move along with the direction of temperature decrease due to thermophoretic forces. Consequently, the decomposition of the produced ammonia (the reverse reaction) can be suppressed at the bottom of the catalyst bed (lower temperature regions). These two examples confirm unique features of the non-equilibrium thermal conditions induced by photo-heating.

2.4 Thermally-enhanced photocatalysis

Thermally-enhanced photocatalysis, which is also known as high-temperature (plasmonic/semiconductor) photocatalysis (Table 1), is designed to exploit the potential of thermal promotions in a photocatalysis-dominated system[54-55]. The temperature has long been investigated as a double-edged sword in conventional solid/gas photocatalysis[15, 56] (Figure 2a). Particularly, photocatalysis under heating can dramatically change the state of the generated charge carriers [57-58] and property of surface intermediate (i.e., redox reaction potential[59], coverage/concentration[60], reactivity[61]). A detrimental role of heating in photocatalysis has often been attributed to the heat-induced desorption of important reactants/reactive species[60], significant nonradiative multiphoton recombination[15] (at a temperature equivalent to and larger than the Debye temperature of the catalyst). Heat is also studied to improve the charge carrier transfer within catalyst[60] and surface reactivity[38]. A temperature-sensitive photocatalytic activity, as displayed in Figure 2b, was often reported over semiconductor-based high-temperature photocatalysis[15, 60]. As demonstrated in the study by Liu et al.[60], an initial increase in photoinduced effect (after subtracting the thermoinduced effect) is obtained in the photocatalytic oxidation of formic acid over TiO_2. This is because that the light and heat work together in surmounting the activation barrier. The charge carrier transfer to reactants is therefore accelerated at elevated temperature. However, the heat-induced suppression in photoactivity was observed at temperatures higher than 125°C. The phenomenon was attributed to the heat-induced O_2 desorption from TiO_2 surface. As listed in Figure 2a, heat-induced suppression and promotion effects would vary from one to another

catalytic system. For that reason, it is critical to identify the optimal temperature range for thermally-enhanced photocatalysis.

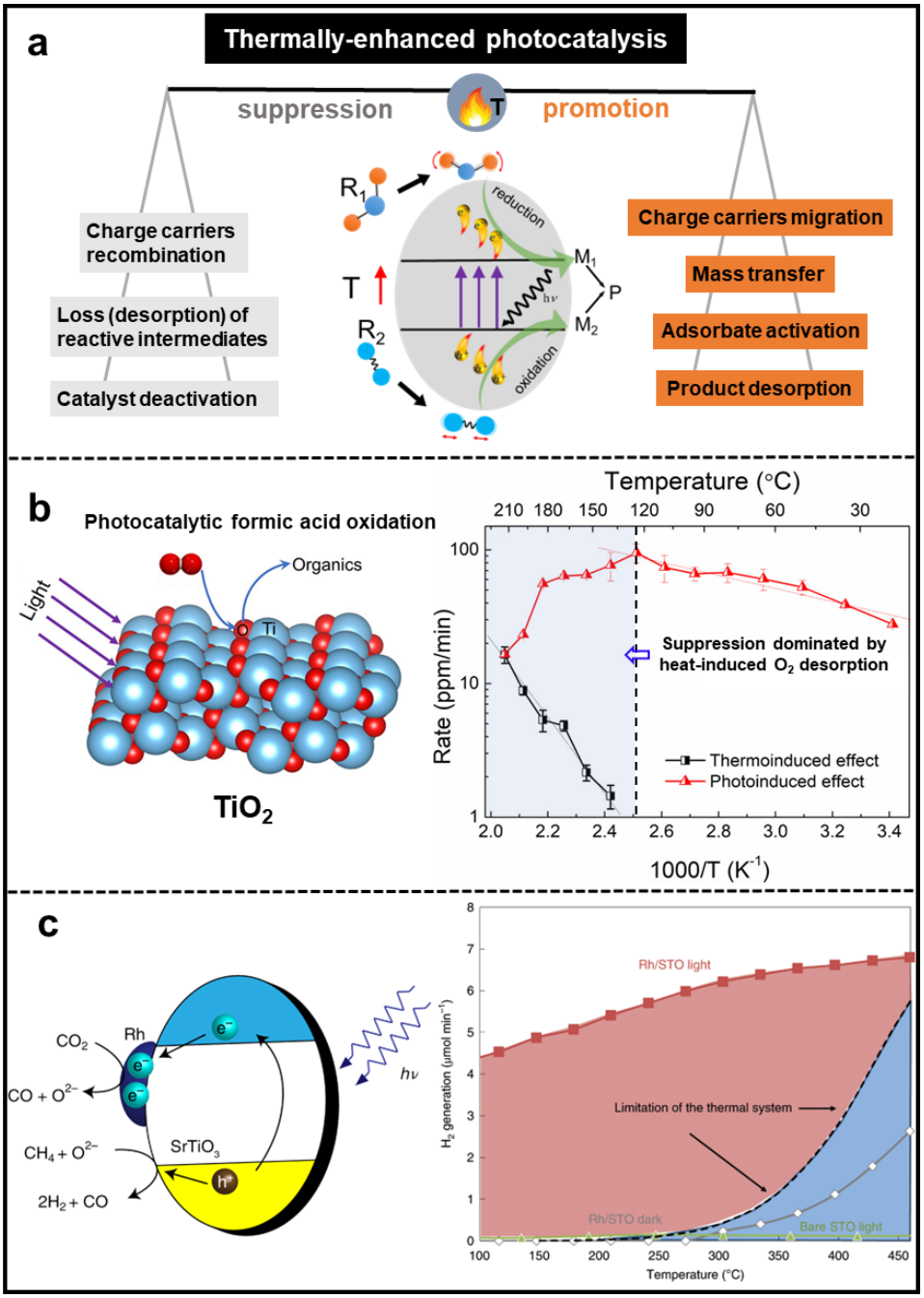

Figure 2. Thermally-enhanced photocatalysis. (a) Schematic illustration of thermally-enhanced photocatalysis and the potential roles of heat (suppression vs. promotion) played in thermally-assisted photocatalysis. (b) Typical temperature-dependent photocatalytic formic oxidation activity over TiO_2 (under UV light illumination). At around 125°C, a transition in the dominant role of heat was shown. The photo-induced effect (red line) was obtained by subtracting thermocatalytic contribution (black line) from overall photocatalytic activity. Reprinted from Ref. [60] Copyright 2019 American Chemical Society. (c) The temperature dependence of DRM activity in dark and light irradiation conditions over Rh/STO. Reprinted with permission from Ref.[62] Copyright 2020 Nature Publishing Group.

Recent studies have revealed the positive role of mild heating in photocatalytic methane activation and conversion. In a report by Miyauchi and co-workers[62] (Figure 2c), Rh supported on $SrTiO_3$ (STO, semiconductor with a bandgap of 3.2 eV) was studied as a substantially high-performance photocatalyst

to drive DRM reaction. In the system, the bandgap excitation of STO played the dominant driving force for the CO_2 and methane activation, on Rh metal (with electrons transferred from STO) and STO (with generated holes), respectively. The temperature played a positive role as evidenced by the increased activity with increasing the temperature (up to 450 °C). An equilibrium-beyond H_2 generation over Rh/STO was achieved when both elevated temperature and light-activation were present. Ye and co-workers[17] studied selective methane oxidation to ethane with oxygen under light-illumination conditions over Au-ZnO/TiO_2 in a fixed-bed flow reactor, where an impressive catalytic performance (>5,000 μmol/g/h production rate with high selectivity 90% towards ethane) was achieved at ≤ 200 °C with a light intensity of 500 mW cm^{-2}. The production of ethane is exclusively derived from direct photo-excitation of the ZnO/TiO_2 hybrid (rather than heating or plasmonic excitation of Au). However, it was emphasised that proper heating (i.e., 140-200 °C) is conducive to the photocatalytic ethane production (for example, providing essential energy for methane activation on catalyst surface and favouring the desorption of methyl radicals into gas phase). Notably, the reported activity is more than one order of magnitude higher than the state-of-the-art photocatalytic system operated at room temperature.

2.5. Photo-enhanced thermocatalysis

Since photoexcited charge carriers can tune or even alter the elementary catalytic steps on thermal catalyst, collective effects of light have been frequently reported to able to help address the limitations known in conventional thermal catalysis (selectivity, equilibrium conversion, etc.). Capabilities of photogenerated electrons/holes in inducing chemical effects and alternating catalytic performance of thermocatalytic system is summarised in Figure 3. Depending on the type of photoexcitation, photo-enhanced thermocatalysis can be divided into mainly three subgroups (see Table 1 and Figure 3a): i) plasmon-enhanced thermocatalysis; ii) bandgap excitation enhanced thermocatalysis; iii) dual/multiple-excitation enhanced thermocatalysis.

To promote the advancement of photo-enhanced thermocatalysis, it has come to a central point to study how photo-generated charge carriers could affect/change the surface chemical properties of the catalyst[63] and/or the intermediary reaction steps[61] compared to that at only heating conditions. In this case, the investigation of electron transfer pathway, and its corresponding disturbance on catalyst surface state and adsorbates becomes critical for the explanation of the observed photothermal activity and overall reaction mechanism. Advanced computational calculations could shed light on physics of charge transfer, for example, at metal@adsorbate interface, at microscopic length scales and ultrafast time scales. For example, the so-called ΔSCF-DFT was used to study the effect of a hot electron transferred to a reactant O_2 molecule[27]. Experimental strategies have been successfully implemented to study the consequences of the charge transfer or energy deposition process. To elucidate the reaction mechanism of the photo-assisted CO_2 hydrogenation over Ni-based catalyst, Tan et al. used in-situ isotopic spectroscopy that can track the kinetics of photo-assisted intermediatory steps and found that photo-activation of the formate species enables an eightfold photo-enhancement on the studied Ni catalyst[61]. In-situ UV-vis has been used to detect the change of Cu state during illumination[63].

As a classic example of plasmon-enhanced thermocatalysis, Christopher et al.[25, 27] investigated visible light-enhanced catalytic ethylene oxidation reactions on plasmonic silver nanostructure and discovered several unique roles of plasmonic excitation in conventional metal-catalysed thermocatalysis. A significant rate enhancement (Figure 3b) was observed under visible light illumination in the range of temperature typical for thermocatalytic ethylene epoxidation over Ag[64]. Light favourably promotes the kinetically sluggish oxygen-activation steps through electron-mediated energy deposition into O_2 antibonding orbitals, which is a rate-determining step in the thermal reaction. Typically, an exponential increase in reaction rate with the operating temperature was observed. In addition, an exceptional

transition from linear to super-linear dependence (rate $\propto$ intensity^n, n>1) of reaction rate on light intensity occurred at ~ 300 mW/cm^{-2}. This has been correlated to a transition from single-electron to multi-electron driven process where one adsorbate can be electronically excited multiple times before overcoming the reaction activation barrier. Significantly, the positive relation between reaction rate/quantum efficiency and operating temperature opens a new venue for more efficient chemical synthesis by coupling thermal activation with plasmon-induced chemistries. Similarly, Halas and co-workers demonstrated the ability of plasmonic excitation (under illumination) in accelerating selective methane dehydrogenation over Cu-Ru catalysts under heating (e.g., 850 K) in DRM reaction (Figure 3c)[65]. The improved selectivity in light-coupled system has been attributed to the accelerated associative H_2 desorption via desorption induced by electronic transitions mechanism (DIET) and the effective removal of deposited carbon. A significant increase in methane conversion is achieved in the coupled system compared to that under only heat (e.g., from 20% to 35% at 850 K). The quantum efficiency also reached a value of 15% at 16 W/cm^{-2} light intensity.

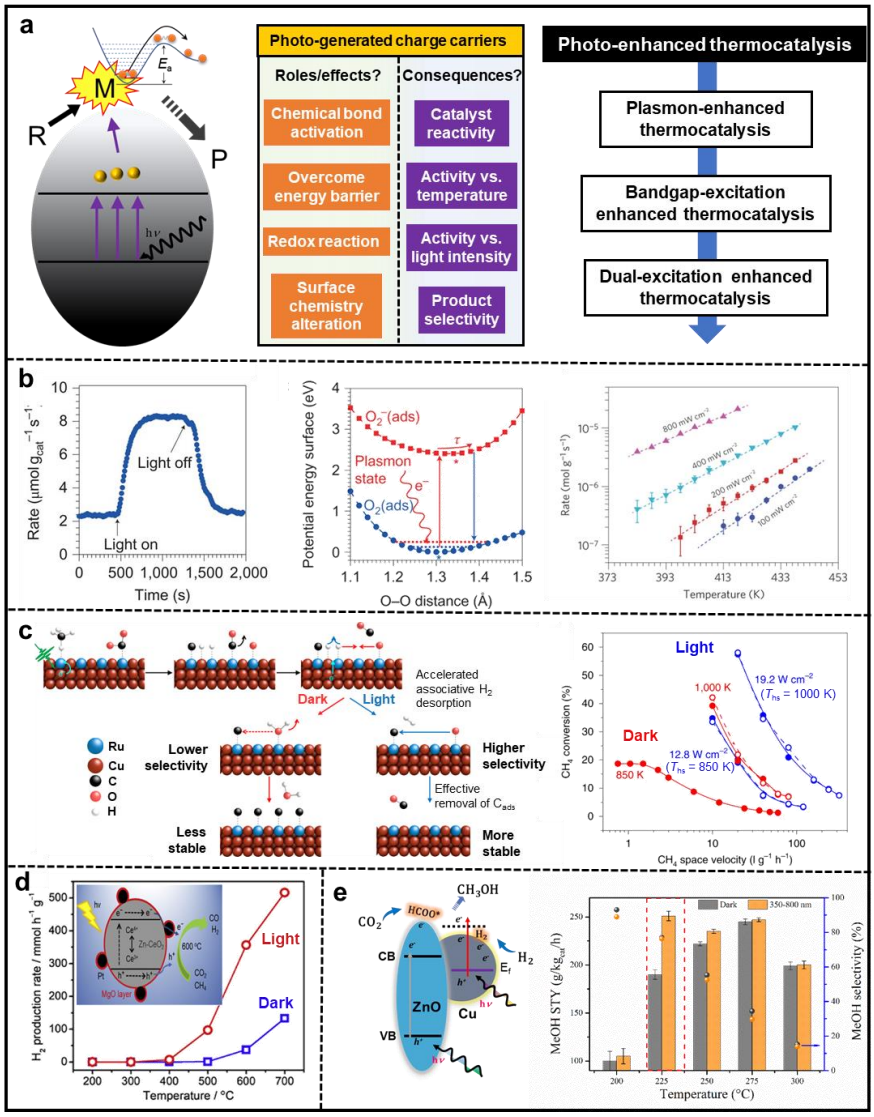

Figure 3. Photo-enhanced thermocatalysis. (a) Schematic illustration of photo-enhanced thermocatalysis and the potential roles of photogenerated charge carriers played in thermocatalysis and their consequences on catalyst performance and activity relationships. Photo-enhanced thermocatalysis can be classified into (b-c) plasmon-enhanced, (d) bandgap excitation enhanced, and (e) dual-excitation enhanced thermocatalysis. (b, left) The rate

of ethylene epoxidation over Ag nanostructure with visible light on and off at 450 K. (b, middle) DFT calculated potential energy surface shows that the excitation of silver surface plasmons allows for the transfer of an excited electron to O_2, forming negatively charged O_2^-, where nuclear motion and bond elongation are induced based on. τ depicts the progression of the O_2 molecule on the negative ion potential energy surface as a function of time. (b, right) photocatalytic reaction rate (log scale) as a function of operating temperature for various light intensities. Reprinted with permission from Ref.[27] Copyright 2011 and Ref.[25]. Copyright 2012 Nature Publishing Group. (c, left) Schematics of enhanced selectivity and stability in photocatalysis via the desorption induced by electronic transitions mechanism (DIET). (c, right) Methane conversion by photothermal catalysis (with light) and thermocatalysis (under dark) as a function of space velocity/temperature over plasmonic Ru-Cu nanoparticles. Filled and unfilled circles represent the measurements of two different batches for a specific condition. Reprinted with permission from Ref.[65] Copyright 2020 Nature Publishing Group. (d) H_2 and CO production rate for DRM reaction over MgO/Pt/Zn-CeO_2 catalyst at low-temperature region in the dark and under light irradiation. Inset shows the bandgap-excitation enhanced DRM reaction mechanism over designed MgO/Pt/Zn-CeO_2 structure. Reprinted with permission from Ref.[40] Copyright 2019 Elsevier Ltd. (e) Dual-excitation (ZnO bandgap and Cu plasmonic excitation) applied for light-enhanced methanol production from CO_2 over industrially relevant Cu/ZnO/Al_2O_3 catalyst. (e, left) Illustration of generated electrons (from Cu and ZnO) acting to activate important catalytic steps (i.e., HCOO* and H_2 relevant) during CO_2 hydrogenation to methanol. (e, right) MeOH selectivity/space time yield (STY) at 200–300 °C under dark and 350–800 nm light irradiation (red dotted box indicates the highest photo-enhancement at 225 °C). Reprinted with permission from Ref.[41] Copyright 2020 Nature Publishing Group.

Strong interactions between thermally-induced process and bandgap excitation[40] or even dual/multi-excitation[41-42] could also occur in photo-enhanced thermocatalysis (detailed in Table 1). Li and co-workers constructed an efficient hybrid CO_2 reforming of CH_4 system over MgO/Pt/Zn-CeO_2 by the integration of bandgap excitation and thermocatalytic effects[40]. As shown in Figure 3d, a significant enhancement in H_2 production was observed under light (i.e., increased to 88 times at 500°C) at reaction temperatures ranging from 500 to 700 °C. The impressive activity (i.e. 97 mmol/$g_{cat.}$/h H_2 produced at 500 °C) was attributed to the Zn-doping and surface MgO coating that acted to improve the separation of charge carriers under light illumination (inset of Figure 7c). Similarly, Hu and co-workers reported an impressive quantum efficiency of 32.3% at 550 °C and 57.8% at 650 °C for photo-enhanced DRM over black TiO_2 supported Pt catalyst[66]. In another work by Xie et al.[41], the ZnO band-gap excitation and Cu plasmonic excitation were found to cooperatively promote methanol-production at the interfacial perimeter of catalyst (Figure 3e). When irradiated with 350–800 nm light, discernible photo-enhancement in methanol production (up to 30%) was observed at 200-250 °C.

In addition to their direct role in facilitating the activation of chemical bonds and surrounding reaction energy barrier, the produced charge carriers can induce alterations in the catalyst's surface state through redox reaction[41, 63] or the creation of defects[67], thus indirectly affecting (improving) catalytic activities. These observed light-induced non-thermal effects correlate closely to the fate of the photogenerated electrons in the studied catalyst system as discussed in section 2.1. The exploration of these intricate light-induced nonthermal effects has emerged as a significant and demanding area of research, as it lays the foundation for the understanding of light-altered catalytic performance. Essential facets for the mechanistic study of photo-enhanced thermocatalysis is outlined in Table1.

2.6. Photo-thermo cascade catalysis for light-driven chemical synthesis

It is well-known that the activation of species in photochemical scheme is markedly different from that generated with thermal chemistry. However, in some instances, the production of the target product is photochemically inhibited[68]. Moreover, the intermediate species produced by light may not be stabilised on the photocatalyst surface at ambient condition, leading to quenching or desorption (i.e., M_1 desorption to form product P_1 in Figure 4a (Scenario 1)). In principle, a catalyst with elevated surface

reactivity (e.g., under heating) can be designed to stabilise the specific species produced from photocatalytic step to execute the subsequential thermally-driven reactions until the target products are yielded. We here describe a concept for the design of cascade reaction system, which makes use of both the capability of surface reactivity (over catalyst B) and the photogenerated high-energy charge carrier (over catalyst A) to exert photo-thermo catalysis collaboratively.

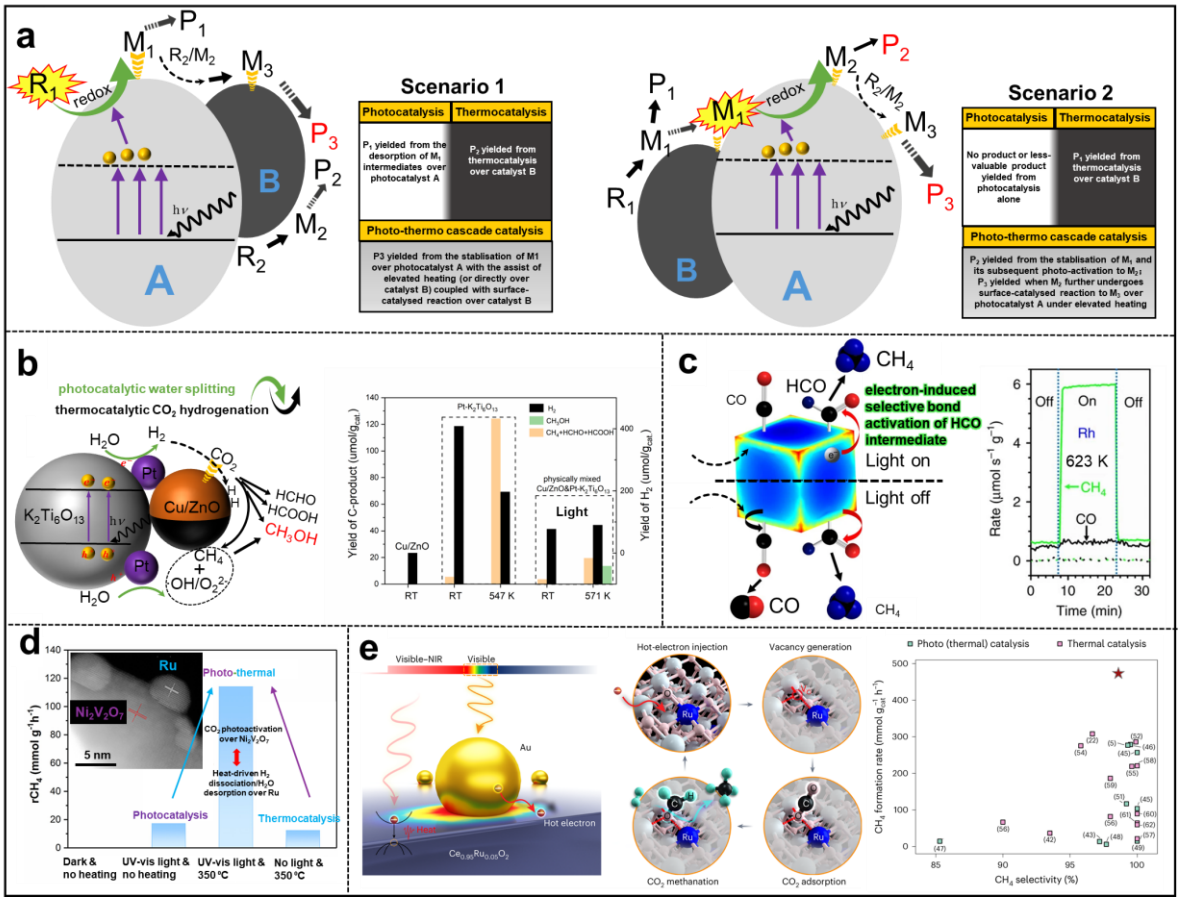

Figure 4. Photo-thermo cascade catalysis for light-driven catalysis. (a) Illustration of photo-thermo cascade catalysis over composite catalyst. A can drive photocatalysis and B can drive thermocatalysis. Under light-heat dual-activation, A and B work collaboratively to drive the whole catalysis process via two typical scenarios where photocatalysis acts to activate reactant or surface-adsorbed intermediates, respectively. In some cases, one bifunctional catalyst can serve as both A and B. R_n, M_n, and P_n refers to reactant, intermediate, and product, respectively. (b) Schematic illustration and activity of the cascade catalysis process for the production of methanol from CO_2 and H_2O over composite structure ($K_2Ti_6O_{13}$ photocatalyst combined with Cu/ZnO catalyst). The illustration was drawn based on the proposed mechanism in the study of Guan et al.[43] Activity data was collected from the study of Guan et al.[43] RT: 300 K. Copyright 2003 Elsevier Ltd. (c) Illustration of coupling surface catalysed CO_2 activation with electron-induced intermediate activation for CO_2 hydrogenation reaction. Right figure shows the rates of CH_4 (green) and CO (black) production at 623 K on Rh/Al_2O_3 (solid lines) and Al_2O_3 (dotted lines) under dark and ultraviolet illumination at 3 W cm^{-2}. Reprinted from ref.[69] Copyright 2017 Nature Publishing Group. (d) Solar-driven CO_2 methanation with over $Ru@Ni_2V_2O_7$ catalyst under different reaction conditions, unprecedented reaction rate was achieved over $Ru@Ni_2V_2O_7$ catalyst in photo-thermo system profiting from the synergism played between $Ni_2V_2V_7$ and Ru in accelerating the elementary catalytic elementary steps (e.g., CO_2 activation, H_2O desorption) in CO_2 methanation reaction. Inset shows the high-resolution image of $Ru@Ni_2V_2O_7$ nanostructure. Reprinted from Ref. [70] Copyright 2021 Elsevier Ltd. (e) Light-driven CO_2 methanation over Au-grafted $Ce_{0.95}Ru_{0.05}O_2$ solid-solution catalysts. The visible–near-infrared light contribute to both the photothermal heating (for initiating reaction) and the hot-electron induced vacancy generation (for promoting reaction). the right figure shows the CO_2 methanation performance

comparison between the $Au_{0.1}/Ce_{0.95}Ru_{0.05}O_2$ and previously reported photothermal and thermal catalyst. Reprinted from Ref.[67] Copyright 2023 Nature Publishing Group.

In an early study in 2003 by Guan et al., the idea of "photo-thermo cascade catalysis" was applied for the reduction of carbon dioxide with water under concentrated sunlight using a hybrid catalyst consisting of a photocatalyst and a conventional CO_2 hydrogenation catalyst (Figure 4b). It is often known that Cu/ZnO can catalyse methanol production at elevated temperatures via CO_2 hydrogenation (CO_2+H_2) but not by CO_2 +H_2O. While photocatalytic CO_2 reduction with H_2O over a semiconductor (or with metal loaded) mainly leads to the formation of CH_4, HCOOH, with a very low selectivity to alcohols. In the study by Guan, Pt-loaded potassium hexatitanate ($K_2Ti_6O_{13}$) is such a photocatalyst that can only produce HCHO/HCOOH from CO_2/H_2O at higher temperatures, no reaction occurs at ambient temperature. When combined with the Cu/ZnO catalyst, the methanol is produced under heat-light dual-activation. Importantly, no methanol can be produced at room temperature under light-only condition over the combined catalyst. It is also mentioned that the H_2 produced from photocatalytic water reduction is indispensable for methanol production, indicating the system will not be able to produce methanol under heat-only condition. Therefore, the studied system is neither a photo-enhanced thermocatalyis nor a thermally-enhanced photocatalysis. Photo-thermo cascade catalysis occurred in the system. For the methanol synthesis, the produced H_2 and CH_4 from photocatalysis over Pt-$K_2Ti_6O_{13}$ were stabilised on the surface and then migrated to participate in the CO_2 hydrogenation and methane oxidation process over the surface of Cu/ZnO for methanol production via thermal catalysis (illustrated in Figure 4b). A cascade strategy was recently proposed to break conventional limitations of methane photocatalytic oxidation by adding a thermo-catalyst and conducting the process in a one-pot reactor[71]. The methane selective conversion into formic acid occurred first over caesium salt of phosphotungstic acid on titania under UV irradiation, which photocatalytically oxidizes methane into a mixture of C_1 oxygenates. These oxygenates are then selectively converted into formic acid over a heterogeneous alumina supported ruthenium catalyst. The methane conversion to formic acid reached a selectivity of 85 % with a high productivity.

As illustrated in Scenario 2 (Figure 4a), although with the reactant (R1) being non-photoactive, photogenerated charge carriers from photocatalyst A can selectively activate the intermediate M1 yielded from thermocatalytic pathway over catalyst B, so that switching the selectivity from P_1 to more valuable products (P_2/P_3). For example, the HCO intermediate is known to be produced from CO_2 hydrogenation reaction over Rh at elevated temperature, which will then lead to the formation of CO and CH_4 product at comparable rate. When excited with when plasmonic Rh is excited by ultraviolet light[69], the product is however shifted to only CH_4. Examination of the band structure (Figure 4c) of Rh catalysts with adsorbed with CHO and CO intermediates (dictating the CO_2 hydrogenation selectivity in the system) suggests that the generated hot electrons tend to interact with the anti-bonding π orbital of C=O bond (at 1-3 eV above fermi level). They contribute to the dissociation of C=O bond of the HCO species, thus facilitating the formation of CH_4. Similarly, the Cu-Co/$SrTiO_3$ catalyst, which appeared to mainly catalyse water gas shift via thermocatalysis (dark, 290 °C. CO_2 produced) and CO methanation reaction via photocatalysis (UV light, ~ 60 °C. CH_4 produced), can be promoted to produce C_2-C_4 hydrocarbons with good selectivity (53.4 %) in photo-thermo cascade system[44]. Within this composite catalyst system, in addition to the intrinsic catalytic activity of Co/Cu towards H_2/CO activation (driven by light-induced heating, ~288 °C), $SrTiO_3$ bandgap excitation and Cu LSPR provide additional charge carriers that could favourably modify/promote intermediatory steps, finally leading to the improved C-C coupling and C_2-C_4 production.

These preliminary and promising findings demonstrate that the integration of two activation processes in photo-thermo cascade catalysis enables driving reactions in a manner surpassing the capabilities of single photocatalysis or thermocatalysis systems. Beyond this synergistic effect, harnessing the diverse

range of light-induced thermal and nonthermal effects allows for the realization of highly efficient light (solar)-driven chemical synthesis (with light being the sole input) within a deliberately engineered photothermal catalyst system. In the study by Li and co-workers[70], the broad-spectrum absorption by the hybrid catalyst (Figure 4d) triggered localized heating at Ru sites (catalyst reaches up to 623K) and bandgap excitation at $Ni_2V_2O_7$, which then contributed to the heat-driven H_2 dissociation/H_2O desorption over Ru and CO_2 photo-activation over $Ni_2V_2O_7$, respectively. Notably, control experiments showed that the cooperative system (illuminated with 300 W Xe lamp) achieved a profound activity enhancement compared to that of system with an individual driving force (6.6 times (vs. photocatalysis) and 9.2 times (vs. thermocatalysis), respectively), confirming a significant synergistic effect between photocatalysis and thermocatalysis (Figure 4b). Accordingly, an unprecedented light-driven CO_2 methanation performance (93.5% CO_2 conversion with 99% selectivity) was achieved over the designed hybrid $Ru/Ni_2V_2O_7$ catalyst.

Taken as another successful example of uniting different light-induced thermal/nonthermal effects, Jiang et al.[67] recently reported a gold-grafted $Ce_{0.95}Ru_{0.05}O_2$ photothermal catalyst for remarkable light-driven CO_2 methanation (Figure 4e). With light of mild intensity (1.6 W/5.3 W cm^{-2}) as the only driving force, CO_2 methanation reaction is initiated by photothermal heating (up to 340 °C) generated on $Ce_{0.95}Ru_{0.05}O_2$ oxide solid solution (with wind range of visible–near-infrared light absorption), on top of that, hot electrons generated from plasmonic Au act to generate abundant Ru-Vo active site to stimulate H_2 dissociation and CO2 methanation. The catalyst tested under high gas velocity (80000 $ml/g_{cat}/h$ with CO_2:H_2=1:4) exhibit CO production rate of 473 $mmol/g_{cat}/h$ which surpass most of the catalysts studied in both thermal and photothermal catalysis systems.

3. Catalyst and reactor design

3.1. Catalyst design for light-heat dual-activation

The existing photothermal catalytic systems are mostly based on either a conventional thermal catalyst (which may have deficient light-harvesting/charge separation ability across the solar spectrum) or a photocatalyst (which may have inferior thermal stability or intrinsic activity at elevated temperatures). The feasibility of coupling two activation pathways over one bifunctional photothermal catalyst could further push the activity/efficiency limit of the catalytic system forward. Solid progress has been achieved in development of photothermal catalyst structure and has been detailed in recent review work[72-75]. Eventually, the designed catalyst for photothermal catalysis will represent a new class of materials different to that of conventional photo-/thermal- catalysts, thus should possess many unique properties/functions:

i) **Catalytically active and light-absorbing.** The intelligent integration of a catalytically active surface with a light-absorbing component constitutes the fundamental criteria for designing innovative photothermal catalysts. Non-costly. Non-costly plasmonic nanostructure with broadband absorption of solar spectrum are expected to play increasingly important role in the design of bifunctional photothermal catalyst. Elevated temperatures are often favoured and required in high performance catalytic synthesis. In photothermal catalysis, optical heating resulted from strong light-matter interaction should be managed and ultilised for thermal-driven process. For example, Nanoporous Titanium nitride (TiN) Metamaterial is studied as plasmonic "nanofurnances" capable of reaching >600 °C under moderately concentrated solar irradiation (~20 Suns, equal to 68% solar-to-heat conversion efficiency)[76]. Furthermore, these plasmonic nanostructure could also generate energetic charge carriers for driving chemical reaction at (adjacent) catalytic active sites[77].

ii) **Nanoscale-resolved heating.** Extensive heating is only required in specific sites (for example, over metal sites for dissociative activation of diatomic molecules, product desorption), while undesired heating can be detrimental for both reaction selectivity and conversion. As discussion in section 2.3, feasible incorporation of light-induced heating can develop highly efficient

catalytic systems where site-specific heating and/or (localised) thermal gradient is engineered to assist endothermic steps in an energy-efficient and thermodynamically favourable way.

iii) **Channelling of charge carrier towards active sites.** Although plasmonic metals are characterized by excellent mobility of charge carriers and high absorption cross-sections[78], they often show very poor activity towards the heterogeneous catalytic reaction. Therefore, the channelling the photogenerated electrons from the plasmonic structure into a catalytically more active component is important in the plasmon-drive catalysis reactions. It is known that, through appropriate materials engineering approaches, the initial energetic charge carriers can be "directed" to the surface or to the catalytically active component (metal or semiconductor) to execute a chemical reaction[19, 79]. Many chemical strategies (e.g., presence of scavengers) have been studied to help extraction of the charge carriers from the excited plasmonic metal to the adsorbate (or to another component then to adsorbate)[19, 79-80]. Furthermore, constructing heterojunctions between two semiconductors has attracted increasing attention due to its thermodynamic and dynamic advantages, which can be a useful strategy for designing efficient photothermal catalysts[81]. In particular, the S-scheme (step-scheme) heterojunction consisting of a reduction photocatalyst (RP) and oxidation photocatalyst (OP) with staggered band structure, offers unique charge transfer pathways that enable prolonged lifetime and strong redox abilities of charge carriers. Thanks to these advantages, S-scheme heterojunction photocatalysts coupled with the photothermal effect have shown exceptional photothermal catalytic CO_2 reduction performance compared to single component photocatalysts[82].

iv) **Cooperative catalysis.** The ultimate goal of photothermal catalysis is to innovatively couple different intermediate steps (either thermally driven or executed by photogenerated charge carriers) in a cooperative and collective way. To that end, essential heating is inputted to raise the average kinetic energy of the molecules and generated charge carriers could assist the steps with a large activation barrier (via electronic excitation[25]). Meanwhile, the feasible coupling between bandgap excitation and plasmonic excitation could be engineered to promote the photocatalytic contribution.

3.2. Reactors for photothermal catalysis

In addition to the catalyst structure, the overall efficacy of the photothermal catalysis is highly dependent on the catalyst packaging and reactor configuration[83].

The prevailing laboratory-scale photothermal reactor system is predominantly adapted from thermochemical setups, incorporating an additional light-permeable window. Both batch-like and flow reactors are commonly employed (depicted in Figure 5a and b). Many of the observed photochemical effects in photo-enhanced thermocatalysis have been investigated by continuously monitoring activity and selectivity under various light conditions within a flow reactor. In-depth mechanistic study utilize this flow system for operando gas-solid experiments, enabling the study of light-induced alterations in surface chemistry and intermediates during the reaction. It is noteworthy that, in the flow system, external heating sources are often necessary to drive reactions at appreciable rates, as the heating effect—especially with low-intensity light—is typically modest. Achieving a substantial contribution from light-induced heating in catalytic reactions necessitates the use of a high-intensity light source and/or closed insulating reactor systems. However, both approaches suffer from limitations in terms of light utilization (constraining the illuminated catalyst region) and efficient energy transfer (effectively delivering heat and light to catalytically active sites).

The prevalent lab-scale photothermal reactor system mainly inherits from the thermochemical system with an extra light-penetrating window. Batch like or flow reactors are commonly used (Figure 5a and b). Most of the identified photochemical effects in the photo-enhanced thermocatalysis were studied through a real-time monitor of activity/selectivity (with/without light illumination) in a flow reactor

system. For the mechanistic study, the flow system is also employed in the operando gas-solid experiments to study the light-altered surface chemistry/intermediates during the reaction. To mention, the external heating source is often required to drive reaction in a noticeable rate as the heating effect (especially with low-intensity light) is often minor in the flow system. To obtain a significant contribution from light-induced heating in the catalytic reaction, a high-intensity light source and/or closed insulating reactor systems were normally employed. However, both systems suffer from poor light utilisation (limited light-illuminating catalyst region) and energy transfer (the delivery of heat/light to catalytically active sites).

Tubular flow-type reactor has an advantage in achieving a high single-pass yield and a high illumination area[84]. If the light is illuminating from the side of the reactor, the use of a compound parabolic concentrator could improve the light uniformity and even incident light intensity[85] (Figure 5d). The use of light-guiding devices (optical fibre[86] or glass rod[87]) is studied as an effective approach for enhancing the light-catalyst interaction. The catalyst is present as a layer of film coated either on the surface of light-guiding material (Figure 5c) or other nanostructured framework. There are two recently announced collaborative projects (in UK[88] and Netherlands[89]) that will be focusing on the investigation and application of light-matter interaction for important chemical reactions. It was proposed in one of the projects that "A 3D network of optical waveguides decorated with plasmonic nanoreactors guided intense light pulses to the catalytically active sites and was embedded in a reaction vessel". In addition, the "shell and tube" reactor (consist of a bunch of tubes mounted inside a cylindrical shell, Figure 5e) system could enable better reactant mixing and mass/energy transfer. More experience can be learnt from the design of optofluidic reactor[90] and thermal flow reactor[91]. Ultimately, the optics and fluids in the system should be integrated in a way that the light-to-chemical efficiency can be maximised.

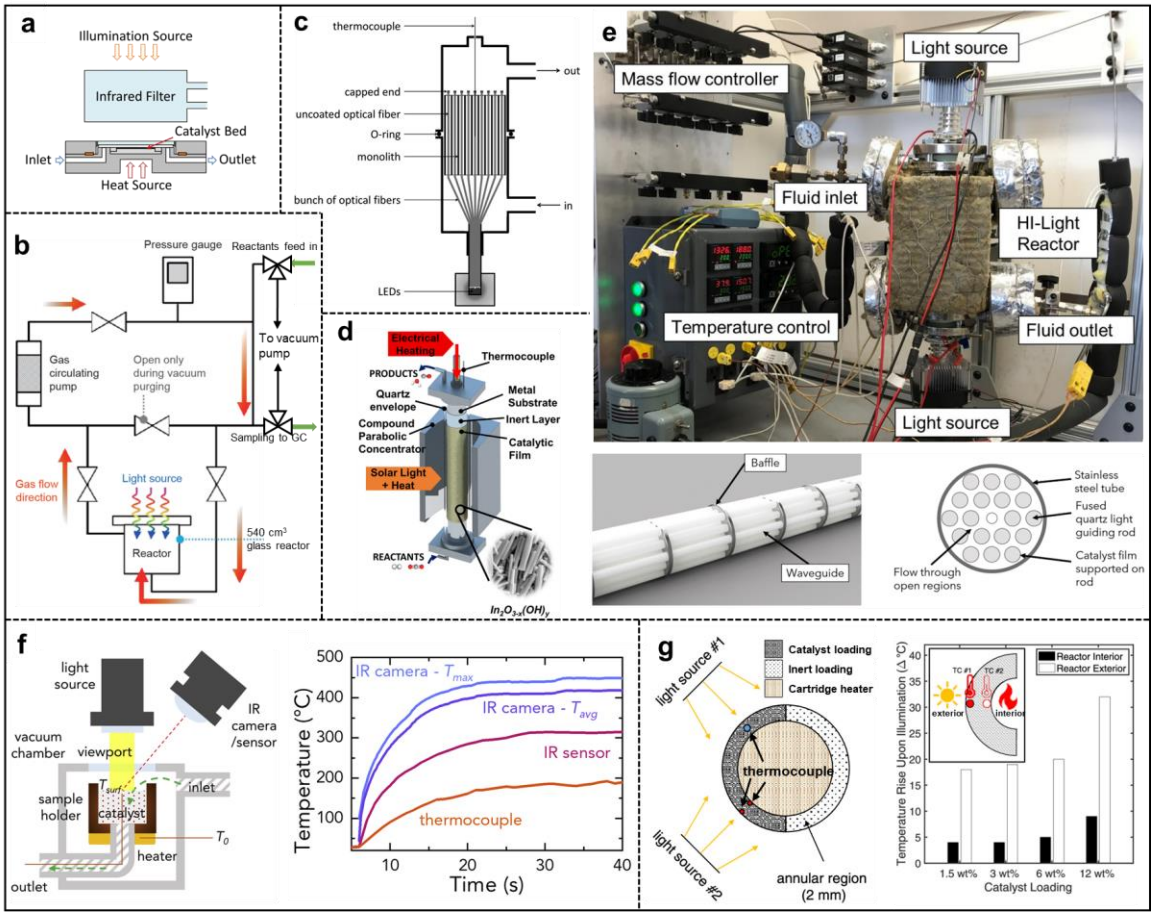

Figure 5. Reactor design and temperature control in photothermal reactor. (a) Flow reactor, reprinted from Ref.[61] Copyright 2020 Nature Publishing Group. (b) Configuration of the batch-type photothermal reactor.

reprinted from Ref. [92] Copyright 2017 Elsevier Ltd. (c) Optical fibre catalytic wall reactor with photocatalyst coated on the surface of the fibres. Reprinted from Ref. [86] Copyright 2014 Elsevier Ltd. (d) Schematic representation of the hybrid photo- and thermal catalytic annular reactors. The catalyst (i.e., $In_2O_{3-x}(OH)_y$) was coated on cylindrical substrates. Reprinted from Ref. [85] Copyright 2020 American Chemical Society. (e) A glass-waveguide-based ''shell-and-tube'' photothermal reactor platform for converting CO_2 to fuels. Left-bottom inset shows baffles were coupled to settle the glass rod as well as to direct the flow pattern inside the reactor, which gives better mixing of the reactants. Right-bottom inset shows the cross-sectional view of the reactor. Reprinted from Ref. [87] Copyright 2020 Elsevier Ltd. (f) Temperature discrepancy measured with different instrumentation. The temperature at the catalyst surface can be monitored by a thermocouple just below the surface and/or by non-contact IR instrumentation viewing the surface from the front viewport. Time-dependent temperature of TiN nanotubes under 17 suns irradiation in air measured by different instrumentation. T_{max} is the maximum temperature measured by the thermal camera, while T_{avg} is the average temperature measured by the same averaged in the area defined by r_{sensor}. Reprinted from Ref. [93] Copyright 2020 Elsevier Ltd. (g) Cross-section view of the reactor dedicated photothermal reactor for accurate temperature and rate activity measurement with. Temperature increase measured under illumination for all four catalyst samples at the reactor interior (closest to the heater, black bars) and exterior (closest to the light source, white bars) under CO oxidation conditions. Reprinted from Ref.[94] Copyright 2022 American Chemical Society.

On the other hand, temperature measurement and regulation in photoreactor is important for the systematic investigation of the photo-/thermo- catalytic performance across the temperature range of interest. Normally, the contribution from heating in light-illuminated system can be evaluated via thermal activity measured under identical external heat supply. Localised heating and thermal gradient across catalyst particles or catalyst bed will emerge when light-generated heating is significant, it then becomes a highly demanding work to elaborate the exact temperature profile of the system. Recent study from Mascaretti et al.[93] pointed out that a significant temperature discrepancy exists between thermocouple and those measured with the IR sensor (Figure 5f), which could lead to large uncertainty in the estimation of key catalytic parameters (i.e., apparent activation energy) and the respective role of heat in the system. Especially, as shown in Figure 5g, dedicated photothermal reactor setup with both outer light-illuminating source and external cartridge inside reactor/catalyst bed was designed by Elias et al.[94] The external heater power was fixed and both the reactor/catalyst interior (closest to the heater) and exterior (closest to the light source) were monitored under CO oxidation conditions. As expected, the extent of measured heating under illumination is more significant directly under the light source (reactor exterior) compared to far from the light source (reactor interior). The accurate in situ catalyst temperature and kinetic reaction rate measurements allow us to scrutinise the local (plasmon-induced activation and localised heating in individual particle) and nonlocal (photothermal equilibrium heating) rate enhancement mechanisms in plasmonic photocatalysis.

4. Conclusion and outlook

Light-driven heterogeneous catalysis via a hybrid light-heat dual-activation pathway is a promising strategy for achieving clean and sustainable energy and chemicals production. In contrast to the exclusive pursuit of pure photocatalysis, which has limited photon utilization efficiency (particularly for visible light range), hybrid light-heat dual-activation, the integration of two distinct activation mechanisms within a single reaction system holds the potential to establish a mutually beneficial scenario. Here, both heat-mediated photochemical process and photo-mediated thermocatalysis can operate concurrently, synergistically enhancing the catalytic reactions.

The potential benefits stemming from the utilization of the light-heat dual-activation approach are outlined below:

- Conducting chemical reactions under milder conditions than in thermocatalysis. The reactions can occur at lower temperatures and with potential use of renewable solar irradiation;

- Enhanced reaction rates are possible due to the synergy of photo and thermo-activation of reacting molecules;
- Generation of thermal gradient across catalyst bed/particle;
- Better selectivity control to target molecules by resonant photoexcitation of specific electronic transition in hybridised substrate-adsorbate orbital states;
- Direct and highly selective synthesis of the molecules over photo-thermo cascade processes. Often direct synthesis of these molecules is impossible to achieve in either pure photo- or thermo-catalysis;
- Higher catalyst stability, small sintering of active phase and reduced carbon deposition via photo-induced desorption.

These advantages collectively underscore the potential of the light-heat dual-activation strategy to revolutionize catalytic processes.

Looking ahead, the landscape of perspectives is set to evolve through the integration of cutting-edge operando characterization techniques and advanced computational calculations. These advancements hold the promise of unveiling deeper insights into two pivotal domains: i) the surface reaction mechanism under dual-activation condition, and ii) sophisticated synergistic effects (between thermochemistry and light-induced chemistries). A new class of bifunctional catalysts, which are capable of effectively harnessing both heat and photogenerated charge carrier for catalytic reaction, is also expected to emerge. Recent developments in optical fibres, optics, lasers, and microstructured reactors with high energy efficiency and fine process control should further improve the delivery of heat and light to catalysts and reacting molecules and thus increasing the efficiency of dual activation of chemical reactions by light and heat. Ultimately, we expect that more record performance in activity/selectivity/energy-efficiency will be achieved in the hybrid systems, which could ultimately lead to a new pathway for sustainable chemicals and fuels production in the future.

Acknowledgement

V.V.O and A.Y.K. acknowledge the support of the French National Research Agency (SolarMethaChem project, ref. ANR-20-SODR-0002). D.H. thanks the China Scholarship Council for a PhD stipend. RA and BX acknowledge the support of the Australian Research Council (ARC) Training Centre for the Global Hydrogen Economy (IC200100023) and ARC Discovery Project (DP230101861).

Competing interests

The authors declare no competing interests.

Corresponding author

Correspondence to Bingqiao Xie or Andrei Y. Khodakov or Rose Amal

References

1. Zimmerman, J. B.; Anastas, P. T.; Erythropel, H. C.; Leitner, W., Designing for a green chemistry future. *Science* **2020,** *367* (6476), 397-400.
2. Lange, J.-P., Performance metrics for sustainable catalysis in industry. *Nature Catalysis* **2021,** *4* (3), 186-192.
3. Li, Y.; Veser, G., Methane and Natural Gas Utilization. *Energy Technol.* **2020,** *8* (8), 2000460.
4. Haynes, C. A.; Gonzalez, R., Rethinking biological activation of methane and conversion to liquid fuels. *Nature Chemical Biology* **2014,** *10* (5), 331-339.
5. Liu, B.; Rajagopal, D., Life-cycle energy and climate benefits of energy recovery from wastes and biomass residues in the United States. *Nature Energy* **2019,** *4* (8), 700-708.
6. Questell-Santiago, Y. M.; Galkin, M. V.; Barta, K.; Luterbacher, J. S., Stabilization strategies in biomass depolymerization using chemical functionalization. *Nature Reviews Chemistry* **2020,** *4* (6), 311-330.
7. Welsby, D.; Price, J.; Pye, S.; Ekins, P., Unextractable fossil fuels in a 1.5 °C world. *Nature* **2021,** *597* (7875), 230-234.
8. Kemfert, C.; Präger, F.; Braunger, I.; Hoffart, F. M.; Brauers, H., The expansion of natural gas infrastructure puts energy transitions at risk. *Nature Energy* **2022,** *7* (7), 582-587.
9. Hu, D.; Ordomsky, V. V.; Khodakov, A. Y., Major routes in the photocatalytic methane conversion into chemicals and fuels under mild conditions. *Appl. Catal., B* **2021,** *286*, 119913.
10. Ravi, M.; Ranocchiari, M.; van Bokhoven, J. A., The Direct Catalytic Oxidation of Methane to Methanol—A Critical Assessment. *Angew. Chem. Int. Ed.* **2017,** *56* (52), 16464-16483.
11. Meng, X.; Cui, X.; Rajan, N. P.; Yu, L.; Deng, D.; Bao, X., Direct Methane Conversion under Mild Condition by Thermo-, Electro-, or Photocatalysis. *Chem* **2019,** *5* (9), 2296-2325.
12. Song, H.; Meng, X.; Wang, Z.-j.; Liu, H.; Ye, J., Solar-Energy-Mediated Methane Conversion. *Joule* **2019,** *3* (7), 1606-1636.
13. Zhao, Y.; Gao, W.; Li, S.; Williams, G. R.; Mahadi, A. H.; Ma, D., Solar- versus Thermal-Driven Catalysis for Energy Conversion. *Joule* **2019,** *3* (4), 920-937.
14. Obee, T. N.; Hay, S. O., Effects of Moisture and Temperature on the Photooxidation of Ethylene on Titania. *Environmental Science & Technology* **1997,** *31* (7), 2034-2038.
15. Westrich, T. A.; Dahlberg, K. A.; Kaviany, M.; Schwank, J. W., High-Temperature Photocatalytic Ethylene Oxidation over TiO_2. *J. Phys. Chem. C* **2011,** *115* (33), 16537-16543.
16. Fu, X.; Clark, L. A.; Zeltner, W. A.; Anderson, M. A., Effects of reaction temperature and water vapor content on the heterogeneous photocatalytic oxidation of ethylene. *Journal of Photochemistry and Photobiology A: Chemistry* **1996,** *97* (3), 181-186.
17. Song, S.; Song, H.; Li, L.; Wang, S.; Chu, W.; Peng, K.; Meng, X.; Wang, Q.; Deng, B.; Liu, Q.; Wang, Z.; Weng, Y.; Hu, H.; Lin, H.; Kako, T.; Ye, J., A selective Au-ZnO/TiO2 hybrid photocatalyst for oxidative coupling of methane to ethane with dioxygen. *Nat. Catal.* **2021**.
18. Zhang, X.; Fan, Y.; You, E.; Li, Z.; Dong, Y.; Chen, L.; Yang, Y.; Xie, Z.; Kuang, Q.; Zheng, L., MOF encapsulated sub-nm Pd skin/Au nanoparticles as antenna-reactor plasmonic catalyst for light driven CO2 hydrogenation. *Nano Energy* **2021,** *84*, 105950.
19. Linic, S.; Chavez, S.; Elias, R., Flow and extraction of energy and charge carriers in hybrid plasmonic nanostructures. *Nat. Mater.* **2021,** *20* (7), 916-924.
20. Robatjazi, H.; Yuan, L.; Yuan, Y.; Halas, N. J., Heterogeneous Plasmonic Photocatalysis: Light-Driven Chemical Reactions Introduce a New Approach to Industrially-Relevant Chemistry. In *Emerging Trends in Chemical Applications of Lasers*, American Chemical Society: 2021; Vol. 1398, pp 363-387.
21. Seemala, B.; Therrien, A. J.; Lou, M.; Li, K.; Finzel, J. P.; Qi, J.; Nordlander, P.; Christopher, P., Plasmon-Mediated Catalytic O2 Dissociation on Ag Nanostructures: Hot Electrons or Near Fields? *ACS Energy Lett.* **2019,** *4* (8), 1803-1809.
22. Lindstrom, C.; Zhu, X.-Y., Photoinduced electron transfer at molecule− metal interfaces. *Chem. Rev.* **2006,** *106* (10), 4281-4300.

23. Zhang, Y.; He, S.; Guo, W.; Hu, Y.; Huang, J.; Mulcahy, J. R.; Wei, W. D., Surface-Plasmon-Driven Hot Electron Photochemistry. *Chemical Reviews* **2018,** *118* (6), 2927-2954.
24. Kazuma, E.; Jung, J.; Ueba, H.; Trenary, M.; Kim, Y., Direct Pathway to Molecular Photodissociation on Metal Surfaces Using Visible Light. *J. Am. Chem. Soc.* **2017,** *139* (8), 3115-3121.
25. Christopher, P.; Xin, H.; Marimuthu, A.; Linic, S., Singular characteristics and unique chemical bond activation mechanisms of photocatalytic reactions on plasmonic nanostructures. *Nat. Mater.* **2012,** *11* (12), 1044.
26. Mukherjee, S.; Libisch, F.; Large, N.; Neumann, O.; Brown, L. V.; Cheng, J.; Lassiter, J. B.; Carter, E. A.; Nordlander, P.; Halas, N. J., Hot Electrons Do the Impossible: Plasmon-Induced Dissociation of H_2 on Au. *Nano Lett.* **2013,** *13* (1), 240-247.
27. Christopher, P.; Xin, H.; Linic, S., Visible-light-enhanced catalytic oxidation reactions on plasmonic silver nanostructures. *Nat. Chem.* **2011,** *3*, 467.
28. Kale, M. J.; Avanesian, T.; Xin, H.; Yan, J.; Christopher, P., Controlling Catalytic Selectivity on Metal Nanoparticles by Direct Photoexcitation of Adsorbate–Metal Bonds. *Nano Lett.* **2014,** *14* (9), 5405-5412.
29. Mascaretti, L.; Schirato, A.; Montini, T.; Alabastri, A.; Naldoni, A.; Fornasiero, P., Challenges in temperature measurements in gas-phase photothermal catalysis. *Joule* **2022**.
30. Keller, E. L.; Frontiera, R. R., Ultrafast Nanoscale Raman Thermometry Proves Heating Is Not a Primary Mechanism for Plasmon-Driven Photocatalysis. *ACS Nano* **2018,** *12* (6), 5848-5855.
31. Boerigter, C.; Campana, R.; Morabito, M.; Linic, S., Evidence and implications of direct charge excitation as the dominant mechanism in plasmon-mediated photocatalysis. *Nat. Commun.* **2016,** *7*, 10545.
32. Baffou, G.; Bordacchini, I.; Baldi, A.; Quidant, R., Simple experimental procedures to distinguish photothermal from hot-carrier processes in plasmonics. *Light: Science & Applications* **2020,** *9* (1), 108.
33. Geng, Z.; Yu, Y.; Offen, A. J.; Liu, J., Achieving maximum overall light enhancement in plasmonic catalysis by combining thermal and non-thermal effects. *Nat. Catal.* **2023**.
34. Cai, M.; Wu, Z.; Li, Z.; Wang, L.; Sun, W.; Tountas, A. A.; Li, C.; Wang, S.; Feng, K.; Xu, A.-B.; Tang, S.; Tavasoli, A.; Peng, M.; Liu, W.; Helmy, A. S.; He, L.; Ozin, G. A.; Zhang, X., Greenhouse-inspired supra-photothermal CO2 catalysis. *Nat. Energy* **2021**.
35. Li, X.; Zhang, X.; Everitt, H. O.; Liu, J., Light-Induced Thermal Gradients in Ruthenium Catalysts Significantly Enhance Ammonia Production. *Nano Lett.* **2019,** *19* (3), 1706-1711.
36. Wang, Y.; Zhang, X.; Chang, K.; Zhao, Z.; Huang, J.; Kuang, Q., MOF Encapsulated AuPt Bimetallic Nanoparticles for Improved Plasmonic-induced Photothermal Catalysis of CO2 Hydrogenation. *Chem. Eur. J.* **2022,** *28* (16), e202104514.
37. Li, Y.; Wen, M.; Wang, Y.; Tian, G.; Wang, C.; Zhao, J., Plasmonic Hot Electrons from Oxygen Vacancies for Infrared Light-Driven Catalytic CO2 Reduction on Bi2O3−x. *Angew. Chem. Int. Ed.* **2021,** *60* (2), 910-916.
38. Wang, L.; Dong, Y.; Yan, T.; Hu, Z.; Jelle, A. A.; Meira, D. M.; Duchesne, P. N.; Loh, J. Y. Y.; Qiu, C.; Storey, E. E.; Xu, Y.; Sun, W.; Ghoussoub, M.; Kherani, N. P.; Helmy, A. S.; Ozin, G. A., Black indium oxide a photothermal CO_2 hydrogenation catalyst. *Nat. Commun.* **2020,** *11* (1), 2432.
39. Luo, S.; Lin, H.; Wang, Q.; Ren, X.; Hernández-Pinilla, D.; Nagao, T.; Xie, Y.; Yang, G.; Li, S.; Song, H.; Oshikiri, M.; Ye, J., Triggering Water and Methanol Activation for Solar-Driven H2 Production: Interplay of Dual Active Sites over Plasmonic ZnCu Alloy. *J. Am. Chem. Soc.* **2021**.
40. Pan, F.; Xiang, X.; Du, Z.; Sarnello, E.; Li, T.; Li, Y., Integrating photocatalysis and thermocatalysis to enable efficient CO_2 reforming of methane on Pt supported CeO_2 with Zn doping and atomic layer deposited MgO overcoating. *Appl. Catal., B* **2020,** *260*, 118189.
41. Xie, B.; Wong, R. J.; Tan, T. H.; Higham, M.; Gibson, E. K.; Decarolis, D.; Callison, J.; Aguey-Zinsou, K.-F.; Bowker, M.; Catlow, C. R. A.; Scott, J.; Amal, R., Synergistic ultraviolet and visible light photo-activation enables intensified low-temperature methanol synthesis over copper/zinc oxide/alumina. *Nat. Commun.* **2020,** *11* (1), 1615.

42. Yu, X.; Yang, L.; Xuan, Y.; Liu, X. L.; Zhang, K., Solar-driven low-temperature reforming of methanol into hydrogen via synergetic photo- and thermocatalysis. *Nano Energy* **2021,** *84*, 105953.
43. Guan, G.; Kida, T.; Harada, T.; Isayama, M.; Yoshida, A., Photoreduction of carbon dioxide with water over K2Ti6O13 photocatalyst combined with Cu/ZnO catalyst under concentrated sunlight. *Appl. Catal., A* **2003,** *249* (1), 11-18.
44. Ning, S.; Sun, Y.; Ouyang, S.; Qi, Y.; Ye, J., Solar Light-induced Injection of Hot Electrons and Photocarriers for Synergistically Enhanced Photothermocatalysis Over Cu-Co/SrTiO3 Catalyst Towards Boosting CO Hydrogenation Into C2–C4 Hydrocarbons. *Appl. Catal., B* **2022**, 121063.
45. Ghoussoub, M.; Xia, M.; Duchesne, P. N.; Segal, D.; Ozin, G., Principles of photothermal gas-phase heterogeneous CO_2 catalysis. *Energy Environ. Sci.* **2019**.
46. Zhao, J.; Guo, X.; Shi, R.; Waterhouse, G. I. N.; Zhang, X.; Dai, Q.; Zhang, T., NiFe Nanoalloys Derived from Layered Double Hydroxides for Photothermal Synergistic Reforming of CH4 with CO2. *Adv. Funct. Mater.* **2022,** *32* (31), 2204056.
47. Peng, Y.; Albero, J.; Franconetti, A.; Concepción, P.; García, H., Visible and NIR Light Assistance of the N2 Reduction to NH3 Catalyzed by Cs-promoted Ru Nanoparticles Supported on Strontium Titanate. *ACS Catal.* **2022,** *12* (9), 4938-4946.
48. Bai, X.; Yuan, D.; Li, Y.; Song, H.; Lu, Y.; San, X.; Lu, J.; Fu, G.; Wang, S.; Ye, J., Ambient sunlight-driven photothermal methanol dehydrogenation for syngas production with 32.9 % solar-to-hydrogen conversion efficiency. *iScience* **2021,** *24* (2), 102056.
49. Li, Y.; Hao, J.; Song, H.; Zhang, F.; Bai, X.; Meng, X.; Zhang, H.; Wang, S.; Hu, Y.; Ye, J., Selective light absorber-assisted single nickel atom catalysts for ambient sunlight-driven CO_2 methanation. *Nat. Commun.* **2019,** *10* (1), 2359.
50. Zhou, L.; Swearer, D. F.; Zhang, C.; Robatjazi, H.; Zhao, H.; Henderson, L.; Dong, L.; Christopher, P.; Carter, E. A.; Nordlander, P., Quantifying hot carrier and thermal contributions in plasmonic photocatalysis. *Science* **2018,** *362* (6410), 69-72.
51. Hu, S.; Liu, B.-J.; Feng, J.-M.; Zong, C.; Lin, K.-Q.; Wang, X.; Wu, D.-Y.; Ren, B., Quantifying Surface Temperature of Thermoplasmonic Nanostructures. *Journal of the American Chemical Society* **2018,** *140* (42), 13680-13686.
52. Mao, C.; Li, H.; Gu, H.; Wang, J.; Zou, Y.; Qi, G.; Xu, J.; Deng, F.; Shen, W.; Li, J.; Liu, S.; Zhao, J.; Zhang, L., Beyond the Thermal Equilibrium Limit of Ammonia Synthesis with Dual Temperature Zone Catalyst Powered by Solar Light. *Chem* **2019,** *5* (10), 2702-2717.
53. Jollans, T.; Caldarola, M.; Sivan, Y.; Orrit, M., Effective Electron Temperature Measurement Using Time-Resolved Anti-Stokes Photoluminescence. *The Journal of Physical Chemistry A* **2020,** *124* (34), 6968-6976.
54. Sun, M.; Zhao, B.; Chen, F.; Liu, C.; Lu, S.; Yu, Y.; Zhang, B., Thermally-assisted photocatalytic CO2 reduction to fuels. *Chemical Engineering Journal* **2021,** *408*, 127280.
55. Nair, V.; Muñoz-Batista, M. J.; Fernández-García, M.; Luque, R.; Colmenares, J. C., Thermo-Photocatalysis: Environmental and Energy Applications. **2019,** *12* (10), 2098-2116.
56. Liu, B.; Zhao, X.; Terashima, C.; Fujishima, A.; Nakata, K., Thermodynamic and kinetic analysis of heterogeneous photocatalysis for semiconductor systems. *Phys. Chem. Chem. Phys.* **2014,** *16* (19), 8751-8760.
57. Zhang, J.; Li, Y.; Sun, J.; Chen, H.; Zhu, Y.; Zhao, X.; Zhang, L.-C.; Wang, S.; Zhang, H.; Duan, X., Regulation of energetic hot carriers on Pt/TiO2 with thermal energy for photothermal catalysis. *Appl. Catal., B* **2022,** *309*, 121263.
58. Cho, Y.; Yamaguchi, A.; Uehara, R.; Yasuhara, S.; Hoshina, T.; Miyauchi, M., Temperature dependence on bandgap of semiconductor photocatalysts. *J. Chem. Phys.* **2020,** *152* (23), 231101.
59. Han, B.; Wei, W.; Chang, L.; Cheng, P.; Hu, Y. H., Efficient visible light photocatalytic CO_2 reforming of CH_4. *ACS Catal.* **2015,** *6* (2), 494-497.
60. Liu, B.; Wu, H.; Parkin, I. P., Gaseous Photocatalytic Oxidation of Formic Acid over TiO2: A Comparison between the Charge Carrier Transfer and Light-Assisted Mars–van Krevelen Pathways. *J. Phys. Chem. C* **2019,** *123* (36), 22261-22272.

61. Tan, T. H.; Xie, B.; Ng, Y. H.; Abdullah, S. F. B.; Tang, H. Y. M.; Bedford, N.; Taylor, R. A.; Aguey-Zinsou, K.-F.; Amal, R.; Scott, J., Unlocking the potential of the formate pathway in the photo-assisted Sabatier reaction. *Nat. Catal.* **2020,** *3* (12), 1034-1043.
62. Shoji, S.; Peng, X.; Yamaguchi, A.; Watanabe, R.; Fukuhara, C.; Cho, Y.; Yamamoto, T.; Matsumura, S.; Yu, M.-W.; Ishii, S.; Fujita, T.; Abe, H.; Miyauchi, M., Photocatalytic uphill conversion of natural gas beyond the limitation of thermal reaction systems. *Nat. Catal.* **2020,** *3* (2), 148-153.
63. Marimuthu, A.; Zhang, J.; Linic, S., Tuning Selectivity in Propylene Epoxidation by Plasmon Mediated Photo-Switching of Cu Oxidation State. *Science* **2013,** *339* (6127), 1590-1593.
64. Pu, T.; Tian, H.; Ford, M. E.; Rangarajan, S.; Wachs, I. E., Overview of Selective Oxidation of Ethylene to Ethylene Oxide by Ag Catalysts. *ACS Catalysis* **2019,** *9* (12), 10727-10750.
65. Zhou, L.; Martirez, J. M. P.; Finzel, J.; Zhang, C.; Swearer, D. F.; Tian, S.; Robatjazi, H.; Lou, M.; Dong, L.; Henderson, L., Light-driven methane dry reforming with single atomic site antenna-reactor plasmonic photocatalysts. *Nat. Energy* **2020**, 1-10.
66. Han, B.; Wei, W.; Chang, L.; Cheng, P.; Hu, Y. H., Efficient Visible Light Photocatalytic CO2 Reforming of CH4. *ACS Catal.* **2016,** *6* (2), 494-497.
67. Jiang, H.; Wang, L.; Kaneko, H.; Gu, R.; Su, G.; Li, L.; Zhang, J.; Song, H.; Zhu, F.; Yamaguchi, A.; Xu, J.; Liu, F.; Miyauchi, M.; Ding, W.; Zhong, M., Light-driven CO2 methanation over Au-grafted Ce0.95Ru0.05O2 solid-solution catalysts with activities approaching the thermodynamic limit. *Nat. Catal.* **2023,** *6* (6), 519-530.
68. Poudyal, S.; Laursen, S., Insights into Elevated-Temperature Photocatalytic Reduction of CO_2 by H_2O. *The Journal of Physical Chemistry C* **2018,** *122* (15), 8045-8057.
69. Zhang, X.; Li, X.; Zhang, D.; Su, N. Q.; Yang, W.; Everitt, H. O.; Liu, J., Product selectivity in plasmonic photocatalysis for carbon dioxide hydrogenation. *Nature communications* **2017,** *8*, 14542.
70. Chen, Y.; Zhang, Y.; Fan, G.; Song, L.; Jia, G.; Huang, H.; Ouyang, S.; Ye, J.; Li, Z.; Zou, Z., Cooperative catalysis coupling photo-/photothermal effect to drive Sabatier reaction with unprecedented conversion and selectivity. *Joule* **2021,** *5* (12), 3235-3251.
71. Hu, D.; Addad, A.; Ben Tayeb, K.; Ordomsky, V. V.; Khodakov, A. Y., Thermocatalysis enables photocatalytic oxidation of methane to formic acid at room temperature beyond the selectivity limits. *Cell Reports Physical Science* **2023,** *4* (2), 101277.
72. Lv, C.; Bai, X.; Ning, S.; Song, C.; Guan, Q.; Liu, B.; Li, Y.; Ye, J., Nanostructured Materials for Photothermal Carbon Dioxide Hydrogenation: Regulating Solar Utilization and Catalytic Performance. *ACS Nano* **2023,** *17* (3), 1725-1738.
73. Fang, S.; Hu, Y. H., Thermo-photo catalysis: a whole greater than the sum of its parts. *Chem. Soc. Rev.* **2022,** *51* (9), 3609-3647.
74. Mateo, D.; Cerrillo, J. L.; Durini, S.; Gascon, J., Fundamentals and applications of photo-thermal catalysis. *Chem. Soc. Rev.* **2021,** *50* (3), 2173-2210.
75. Xie, B.; Lovell, E.; Tan, T. H.; Jantarang, S.; Yu, M.; Scott, J.; Amal, R., Emerging material engineering strategies for amplifying photothermal heterogeneous CO2 catalysis. *J. Energy Chem.* **2020,** *59* (1), 108-125.
76. Naldoni, A.; Kudyshev, Z. A.; Mascaretti, L.; Sarmah, S. P.; Rej, S.; Froning, J. P.; Tomanec, O.; Yoo, J. E.; Wang, D.; Kment, Š.; Montini, T.; Fornasiero, P.; Shalaev, V. M.; Schmuki, P.; Boltasseva, A.; Zbořil, R., Solar Thermoplasmonic Nanofurnace for High-Temperature Heterogeneous Catalysis. *Nano Lett.* **2020,** *20* (5), 3663-3672.
77. Rej, S.; Mascaretti, L.; Santiago, E. Y.; Tomanec, O.; Kment, Š.; Wang, Z.; Zbořil, R.; Fornasiero, P.; Govorov, A. O.; Naldoni, A., Determining Plasmonic Hot Electrons and Photothermal Effects during H2 Evolution with TiN–Pt Nanohybrids. *ACS Catal.* **2020,** *10* (9), 5261-5271.
78. Linic, S.; Christopher, P.; Ingram, D. B., Plasmonic-metal nanostructures for efficient conversion of solar to chemical energy. *Nat. Mater.* **2011,** *10* (12), 911-921.
79. Aslam, U.; Chavez, S.; Linic, S., Controlling energy flow in multimetallic nanostructures for plasmonic catalysis. *Nat. Nanotechnol.* **2017,** *12* (10), 1000-1005.

80. Rao, V. G.; Aslam, U.; Linic, S., Chemical Requirement for Extracting Energetic Charge Carriers from Plasmonic Metal Nanoparticles to Perform Electron-Transfer Reactions. *J. Am. Chem. Soc.* **2019,** *141* (1), 643-647.
81. Xu, Q.; Zhang, L.; Cheng, B.; Fan, J.; Yu, J., S-Scheme Heterojunction Photocatalyst. *Chem* **2020,** *6* (7), 1543-1559.
82. Gao, X.; He, H.; Zhu, W.; Yang, C.; Xu, K.; Feng, B.; Hu, Y.; Fu, F., Continuously Flow Photothermal Catalysis Efficiently CO2 Reduction Over S-Scheme 2D/0D Bi5O7I-OVs/Cd0.5Zn0.5S Heterojunction with Strong Interfacial Electric Field. *Small* **2023,** *19* (12), 2206225.
83. Fan, W. K.; Tahir, M., Recent developments in photothermal reactors with understanding on the role of light/heat for CO2 hydrogenation to fuels: A review. *Chem. Eng. J.* **2022,** *427*, 131617.
84. Liu, X.; Xing, C.; Yang, F.; Liu, Z.; Wang, Y.; Dong, T.; Zhao, L.; Liu, H.; Zhou, W., Strong Interaction over Ru/Defects-Rich Aluminium Oxide Boosts Photothermal CO2 Methanation via Microchannel Flow-Type System. *Adv. Energy Mater. n/a* (n/a), 2201009.
85. Mohan, A.; Ulmer, U.; Hurtado, L.; Loh, J.; Li, Y. F.; Tountas, A. A.; Krevert, C.; Chan, C.; Liang, Y.; Brodersen, P.; Sain, M. M.; Ozin, G. A., Hybrid Photo- and Thermal Catalyst System for Continuous CO_2 Reduction. *ACS Appl. Mater. Interfaces* **2020,** *12* (30), 33613-33620.
86. Taboada, E.; Angurell, I.; Llorca, J., Dynamic photocatalytic hydrogen production from ethanol–water mixtures in an optical fiber honeycomb reactor loaded with Au/TiO2. *J. Catal.* **2014,** *309*, 460-467.
87. Cao, X. E.; Kaminer, Y.; Hong, T.; Schein, P.; Liu, T.; Hanrath, T.; Erickson, D., HI-Light: A Glass-Waveguide-Based "Shell-and-Tube" Photothermal Reactor Platform for Converting CO2 to Fuels. *iScience* **2020,** *23* (12), 101856.
88. LCN researcher leads £10million EPSRC grant investigating light-driven energy-conversion. London Centre for Nanotechnology (LCN): 2022.
89. Light-catalyst interactions to sense and steer chemical reactions. Utrecht University: 2022.
90. Erickson, D.; Sinton, D.; Psaltis, D., Optofluidics for energy applications. *Nature Photonics* **2011,** *5* (10), 583-590.
91. Renken, A.; Kiwi-Minsker, L., Chapter 2 - Microstructured Catalytic Reactors. In *Advances in Catalysis*, Gates, B. C.; Knözinger, H., Eds. Academic Press: 2010; Vol. 53, pp 47-122.
92. Kho, E. T.; Jantarang, S.; Zheng, Z.; Scott, J.; Amal, R., Harnessing the Beneficial Attributes of Ceria and Titania in a Mixed-Oxide Support for Nickel-Catalyzed Photothermal CO2 Methanation. *Engineering* **2017,** *3* (3), 393-401.
93. Mascaretti, L.; Schirato, A.; Montini, T.; Alabastri, A.; Naldoni, A.; Fornasiero, P., Challenges in temperature measurements in gas-phase photothermal catalysis. *Joule* **2022,** *6* (8), 1727-1732.
94. Elias, R. C.; Linic, S., Elucidating the Roles of Local and Nonlocal Rate Enhancement Mechanisms in Plasmonic Catalysis. *Journal of the American Chemical Society* **2022,** *144* (43), 19990-19998.